0026-895X/94/040685-08$03.00/0

MOLECULAR PHARMACOLOGY, 46:685-692, 1994.

Identification of Drugs Competing with *d*-Tubocurarine for an Allosteric Site on Cardiac Muscarinic Receptors

MAGALI WAELBROECK

Department of Biochemistry and Nutrition, Medical School, Université Libre de Bruxelles, B-1070 Brussels, Belgium

Received March 18, 1994; Accepted July 22, 1994

SUMMARY

d-Tubocurarine behaved as a weak allosteric inhibitor of *N*-[^{3}H] methylscopolamine binding to cardiac M_2 muscarinic receptors. In a low ionic strength buffer devoid of bivalent ions, *d*-tubocurarine recognized cardiac M_2 receptors in the micromolar concentration range and decreased their affinity for *N*-[^{3}H]methylscopolamine by at most 4-fold. To identify the compounds that preferentially recognize this accessory site (as opposed to the classical muscarinic binding site), we measured the inhibition by different drugs of *N*-[^{3}H]methylscopolamine binding, in the absence or presence of *d*-tubocurarine. The effect of gallamine was competitively inhibited by *d*-tubocurarine; both drugs compete for the same accessory site on muscarinic receptors. The effects of dexetimide, levetimide, 4-diphenylacetoxy-*N*-ethylpiperidine ethobromide, AF-DX 116, and telenzepine on *N*-[^{3}H] methylscopolamine binding were not affected or were barely affected by *d*-tubocurarine; these compounds preferentially recognize another binding site (probably the muscarinic binding site). The dose-effect curves for pentamethylene-bis(4-diphenylacetoxymethylpiperidine) bromide and methoctramine were shifted, but at most 10-fold, by *d*-tubocurarine. It is likely that (in this low ionic strength incubation buffer) methoctramine and pentamethylene-bis(4-diphenylacetoxymethylpiperidine) bromide had comparable affinities for the muscarinic site and the accessory site. *d*-Tubocurarine competitively inhibited their binding to the accessory site and allosterically inhibited their binding to the muscarinic site. This resulted in a large decrease (40–60-fold) of their overall affinity for muscarinic receptors.

Five muscarinic receptor subtypes have been cloned (1). They all belong to the family of receptors that have seven transmembrane helices and activate G proteins. An aspartate residue in the third transmembrane α-helix is essential for receptor recognition by muscarinic agonists and antagonists, confirming the hypothesis that the "classical" muscarinic binding site is situated in a pocket formed by the seven transmembrane helices (see Ref. 1 for review).

Gallamine is a neuromuscular blocking agent. At therapeutic doses, it may antagonize the negative inotropic and chronotropic actions of muscarinic agonists in heart. Its mechanism of action is not competitive; it decreases by 10–300-fold the affinity of muscarinic drugs for cardiac and brain muscarinic receptors (2).

Allosteric interactions are very flexible; allosteric compounds may favor as well as inhibit binding of the natural ligand (acetylcholine) to the primary site. Allosteric sites are therefore very attractive for therapeutic intervention.

After the demonstration that gallamine slows the rate of dissociation of tracer from muscarinic receptors (2), this effect was considered to be the mark of ligands recognizing the allosteric site. A number of drugs have been reported to slow tracer dissociation from cardiac, neuronal, or smooth muscle muscarinic receptors. These include nonselective competitive antagonists like atropine (3) and cocaine (4), cardioselective muscarinic antagonists (5, 6), antiarrythmic agents (7–9), ganglionic and neuromuscular blockers (2, 10–12), acetylcholinesterase inhibitors and reactivators (13–15), K^+ and Ca^{2+} channel blockers (16, 17), protamine (18), and snake toxins (19), as well as the M_1-selective agonist McNeil-A-343 (20).

The large variety of compounds capable of slowing [^{3}H]NMS dissociation led to the hypothesis that different allosteric ligands might act at different sites and that some drugs might have nonspecific effects (see Ref. 3). This is a crucial issue, because if the "allosteric effects" are nonspecific then the possibility for therapeutic applications would be limited.

In a very elegant paper, Ellis and Seidenberg (15) recently demonstrated that the neuromuscular blocking agent gallamine and the acetylcholinesterase reactivator obidoxime slow the [^{3}H]NMS dissociation rate through a common site on cardiac muscarinic receptors. This supports the hypothesis that differ-

This work was supported by Grant 1.5.011.94 F from the Fund for Medical Scientific Research and the Bekales Foundation (Belgium).

ABBREVIATIONS: NMS, *N*-methylscopolamine; AF-DX 116, 11-[2-[(diethylamino)methyl]-1-piperidinyl]acetyl-5,11-dihydro-6*H*-pyrido[2,3-*b*][1,4]benzodiazepine-6-one; *N*-ethyl-4-DAMP, 4-diphenylacetoxy-*N*-ethylpiperidine ethobromide; bispentamethylene-4-DAMP, pentamethylene-bis(4-diphenylacetoxymethylpiperidine) bromide; IC_{35}, drug concentration inhibiting tracer binding to 35% of control.

ent allosteric modulators interact with a common, well defined, allosteric site on the muscarinic receptor. It is, however, quite possible that some of these so-called "allosteric drugs" recognize the classical muscarinic binding site at low concentrations and interact with the allosteric site only at much higher concentrations.

Previous results indicated that *d*-tubocurarine binds to an accessory site on the muscarinic receptor and does not occupy the muscarinic site itself. We took advantage of the fact that *d*-tubocurarine only partially inhibits [^{3}H]NMS binding. We were therefore able to analyze the effect (inhibition of [^{3}H]NMS binding) of several compounds in the presence and in the absence of *d*-tubocurarine. We assumed that, if the compound is an allosteric inhibitor of [^{3}H]NMS binding, then it should compete with *d*-tubocurarine for the accessory site. If this is true, then *d*-tubocurarine should competitively inhibit the effect of the compound (decreased [^{3}H]NMS binding). On the other hand, if the test compound preferentially recognizes the muscarinic binding site, then its binding (by analogy with [^{3}H]NMS) should be little affected by *d*-tubocurarine. It should therefore compete with [^{3}H]NMS almost as well in the absence and in the presence of *d*-tubocurarine.

Experimental Procedures

Chemicals. [*N-methyl*-^{3}H]NMS chloride (84 Ci/mmol) was obtained from Amersham International (Bucks, England). *d*-Tubocurarine chloride and gallamine triethiodide were obtained from Sigma Chemical Co. (St. Louis, MO) and dexetimide and levetimide from Janssen Pharmaceutica (Beerse, Belgium). The following drugs were gifts: AF-DX 116 and telenzepine from Dr. K. Thomae, GmbH (Biberach, Germany); *N*-ethyl-4-DAMP bromide and bispentamethylene-4-DAMP bromide from Dr. R. Barlow (Bristol University, Bristol, UK); and methoctramine from Dr. C. Melchiorre (Bologna, Italy). McN-A-343 was synthesized by Union Chimique Belge Laboratories (Braine-l'Alleud, Belgium), according to published methods.

Cardiac homogenate preparation. Male Wistar albino rats were killed by decapitation, and the heart was immediately removed, rinsed in saline (150 mM NaCl), and then stored in liquid nitrogen until use. Immediately before use, the heart was thawed and homogenized in 20 mM Tris·HCl buffer, pH 7.5, enriched with 250 mM sucrose, for 5 sec with a Ultraturrax homogenizer, followed by seven up and down strokes in a glass-Teflon homogenizer. The homogenate was filtered through two layers of medical gauze and used for binding studies at a final concentration of 200–250 μg of protein/assay.

Binding assays. [^{3}H]NMS binding was measured in 1.2 ml of 10 mM sodium phosphate buffer, pH 7.4. The incubation was stopped by addition of 2 ml of ice-cold 50 mM sodium phosphate buffer and rapid filtration on glass GF/C filters (which had been soaked in 0.01% polyethyleneimine), followed by three rinses with the same buffer. The filters were dried and then counted for radioactivity in a toluene-based liquid scintillation buffer. Nonspecific binding was defined as tracer binding in the presence of 1 μM atropine.

Binding of the allosteric drugs was very sensitive to the addition of divalent cations. We therefore used high performance liquid chromatography-grade deionized water (resistivity of >17 MΩ) for all experiments reported in this work.

Saturation and competition binding assays. For saturation assays, [^{3}H]NMS binding was measured at various tracer concentrations (0.03–2 nM), in the absence or presence of *d*-tubocurarine. For competition curves, [^{3}H]NMS binding was measured at a single high tracer concentration (1 nM = 4 × K_d in this buffer), in the presence of the indicated unlabeled drug concentrations and in the absence or presence of *d*-tubocurarine. The incubation time was increased to 6 hr at 25°, to approach equilibrium binding in the presence of *d*-tubocurarine.

Dissociation kinetics. Cardiac homogenates were preincubated for 1 hr in the presence of 1.0 nM [^{3}H]NMS. Dissociation was induced by the simultaneous addition of 1 μM atropine and the indicated concentrations of the unlabeled drugs. Residual binding was determined 24 min after this addition, by filtration, as indicated above. At 1 μM, atropine saturates the muscarinic binding site but does not recognize the allosteric site (see Discussion).

Data analysis and equations. Let us assume that *d*-tubocurarine (D) can bind only to the accessory site, [^{3}H]NMS (N*) can bind only to the muscarinic binding site, and the second unlabeled ligand (L) is able to recognize both sites

$$\begin{array}{ccccc} \mathrm{D\,R\,L} & \overset{\alpha_L K_L}{\rightleftarrows} & \mathrm{D\,R} & \overset{\alpha_D K_N}{\rightleftarrows} & \mathrm{D\,R\,N^*} \\ \uparrow & & \uparrow & & \uparrow \\ \alpha_L K_D & & K_D & & \alpha_D K_D \\ \downarrow & & \downarrow & & \downarrow \\ \mathrm{R\,L} & \overset{K_L}{\rightleftarrows} & \mathrm{R} & \overset{K_N}{\rightleftarrows} & \mathrm{R\,N^*} \\ \uparrow & & \uparrow & & \uparrow \\ \alpha_{bis} K_A & & K_A & & \alpha_A K_A \\ \downarrow & & \downarrow & & \downarrow \\ \mathrm{L\,R\,L} & \underset{\alpha_{bis} K_L}{\rightleftarrows} & \mathrm{L\,R} & \underset{\alpha_A K_N}{\rightleftarrows} & \mathrm{L\,R\,N^*} \end{array}$$

If Y represents the fraction of receptors occupied by [^{3}H]NMS, then in the absence of any drug

$$Y_{0,0} = \frac{N^*}{N^* + K_N} \tag{1}$$

where K_N is the tracer dissociation constant, and in the presence of *d*-tubocurarine (D) and another ligand (L)

$$Y_{L,D} = \frac{N^*}{N^* + K'_N(L, D)} \tag{2}$$

with

$$K'_N = K_N \left\{ \frac{1 + \frac{L}{K_A} + \frac{L}{K_L} + \frac{D}{K_D} + \frac{L \cdot D}{\alpha_L K_L D_D} + \frac{L^2}{\alpha_{bis} K_A K_L}}{1 + \frac{D}{\alpha_D K_D} + \frac{L}{\alpha_A K_A}} \right\} \tag{3}$$

K'_N is the apparent tracer dissociation constant in the presence of the ligand and *d*-tubocurarine. It is increased (and tracer binding is decreased) because of 1) binding of the ligand to the accessory site of the "empty" receptor (K_A), 2) binding of the ligand to the muscarinic site of the empty receptor (K_L), 3) binding of *d*-tubocurarine to the accessory site of the empty receptor (K_D), 4) simultaneous binding of the ligand to the muscarinic site and of *d*-tubocurarine to the accessory site ($\alpha_L K_L K_D$), or 5) simultaneous binding of two ligand molecules to the accessory and muscarinic sites of the same receptor ($\alpha_{bis} K_A K_L$). These inhibitory effects are counteracted by 1) binding of *d*-tubocurarine to the accessory site of NMS*-bound receptors ($\alpha_D K_D$) and 2) binding of the ligand to the accessory site of NMS*-bound receptors ($\alpha_K K_A$). All of the constants in these equations are dissociation constants.

It is not possible to identify which binding site is actually occupied by the ligand on the empty receptor (K_A or K_L). We can obtain by curve fitting only an "overall dissociation constant," $(1/K_A + 1/K_L)^{-1} = K_A K_L/(K_A + K_L)$, describing receptor occupancy by a single ligand at either the muscarinic or the accessory site.

The competition curve can be described by

$$\frac{Y_{L,D}}{Y_{0,0}} = \frac{N^*/K_N + 1}{N^*/K_N + K'_N/K_N} \tag{4}$$

where $Y_{L,D}$ is the fraction of receptors occupied by [^{3}H]NMS in the presence of the ligand and *d*-tubocurarine and $Y_{0,0}$ is the fraction of receptors occupied by [^{3}H]NMS in the absence of other drugs.

Results

Value of K_N. The [^{3}H]NMS saturation curves were compatible with the existence of a single site, with a K_N value of 0.25 ± 0.05 nM in this buffer (data not shown).

Effect of *d*-tubocurarine on [^{3}H]NMS dissociation and binding. [^{3}H]NMS dissociated from the cardiac receptors with a single dissociation rate constant (k_{off}), equal to 0.15 ± 0.02 min^{-1} in the absence of *d*-tubocurarine. The dissociation rate was also monophasic, but slower, in the presence of *d*-tubocurarine (0.1 μM to 1 mM) (data not shown).

As shown in Fig. 1A, *d*-tubocurarine at maximally effective concentrations was capable of preventing [^{3}H]NMS dissociation. The concentration necessary for half-maximal inhibition of [^{3}H]NMS dissociation was 2.5 ± 1.0 μM.

After 6 hr of incubation, the *d*-tubocurarine competition curves were shallow, with an IC_{50} value of >500 μM (Fig. 1B). Equilibrium binding was not achieved in the presence of >100 μM *d*-tubocurarine.

The *d*-tubocurarine competition curves obtained in the presence of different [^{3}H]NMS concentrations (0.03, 0.06, 1.0, or 2.0 nM), two of which are shown in Fig. 1, were fitted assuming that *d*-tubocurarine recognizes a single accessory site on the receptor. The average values of K_D and $\alpha_D K_D$ are indicated in Table 1.

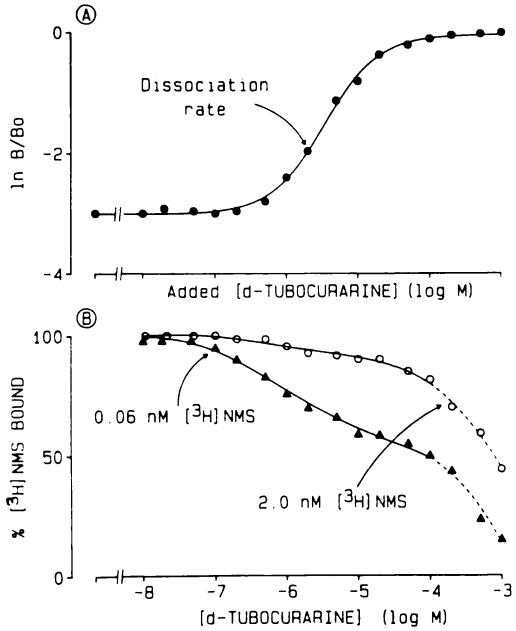

Fig. 1. Dose-effect curves for *d*-tubocurarine effects on the [^{3}H]NMS dissociation rate and [^{3}H]NMS binding. A, Residual [^{3}H]NMS binding was measured 24 min after addition of 1 μM atropine and the indicated *d*-tubocurarine concentrations. B, Binding of 0.06 nM (▲) or 2.0 nM (○) [^{3}H]NMS was measured after 6 hr of incubation in the absence or presence of the indicated *d*-tubocurarine concentrations. Data are representative of two experiments. The residual [^{3}H]NMS binding data are plotted on a logarithmic scale, because this is more representative of the dissociation rate constant, k_{off}. The residual tracer binding in the presence of 1 μM atropine alone was 5% in this experiment. The *d*-tubocurarine competition curves shown in this experiment were fitted with K_D = 1 μM and $\alpha_D K_D$ = 2.5 μM. The average values of K_D and $\alpha_D K_D$ (15 experiments) were 0.72 ± 0.13 μM and 2.5 ± 0.22 μM, respectively.

Inhibition by the other compounds of [^{3}H]NMS binding and [^{3}H]NMS dissociation. Telenzepine (Fig. 2), AF-DX 116 (Fig. 3), *N*-ethyl-4-DAMP and bispentamethylene-4-DAMP (Fig. 4), and dexetemide (Fig. 5) completely inhibited [^{3}H]NMS binding, with Hill coefficients close to 1 (Table 2). As generally observed with muscarinic agonists, the McN-A-343 competition curves were shallow (Hill coefficient of <1) (Fig. 2; Table 2). After 2-hr incubations, a plateau was observed at concentrations above 50 μM and [^{3}H]NMS binding was not prevented even by 1 mM McNeil-A-343 (Fig. 2). Gallamine inhibited [^{3}H]NMS binding. However, even at concentrations up to 1 mM (Fig. 3) it was unable to completely prevent [^{3}H]NMS binding. The Hill coefficient of the competition curve was less than 1 (Table 2). Methoctramine (Fig. 3) inhibited [^{3}H]NMS binding completely, with a Hill coefficient slightly greater than 1 (Table 2). Levetimide (Fig. 5) inhibited [^{3}H]NMS binding completely, with a Hill coefficient slightly smaller than 1 (Table 2).

All of the compounds investigated were capable of decreasing the [^{3}H]NMS dissociation rate. To ensure that the [^{3}H]NMS dissociation rate was monophasic also in the presence of all of the compounds, we measured the dose-dependent inhibition of [^{3}H]NMS binding after either 10 min or 24 min of dissociation. The ln (B/B_o) value was proportional to the dissociation interval at every drug concentration tested. Assuming that the compounds could all prevent [^{3}H]NMS dissociation, we obtained EC_{50} values between 0.1 and 0.2 mM for all of the compounds with a single positive charge (telenzepine, McNeil-A-343, AF-DX 116, *N*-ethyl-4-DAMP, dexetimide, and levetimide) and EC_{50} values between 0.5 and 1.0 μM for all of the compounds with at least two cationic groups [gallamine (3+), bispentamethylene-4-DAMP (2+), and methoctramine (4+)] (Table 2). All of the dose-effect curves were compatible with mass action (Hill coefficient of 1) (Table 2).

[^{3}H]NMS binding inhibition by benzetemide (dexetemide and levetimide) was very stereoselective. In contrast, the two enantiomers decreased the [^{3}H]NMS dissociation rates with similar potencies (Fig. 5; Table 2).

Effect of *d*-tubocurarine on the competition curves. As shown in Figs. 6-8, in the presence of *d*-tubocurarine [^{3}H]NMS binding was less inhibited by high concentrations of gallamine, methoctramine, or bispentamethylene-4-DAMP. We systematically observed a slightly smaller shift of the methoctramine or bispentamethylene-4-DAMP competition curves, compared with the gallamine competition curve, in the presence of 100 μM *d*-tubocurarine (Figs. 6–8). The gallamine concentration necessary to inhibit [^{3}H]NMS binding to 35% of the control value (IC_{35}) increased linearly with the *d*-tubocurarine concentration (Fig. 6B). In contrast, the IC_{35} values of bispentamethylene-4-DAMP and methoctramine reached maximum values between 30 and 100 μM *d*-tubocurarine (Figs. 7B and 8B). At high concentrations, all of the compounds with a single positive charge (Figs. 9 and 10) inhibited [^{3}H]NMS binding to a similar extent in the absence and in the presence of 100 μM *d*-tubocurarine.

It is essential to allow tracer binding to reach equilibrium for a quantitative analysis of the binding data. Equilibrium binding should, by definition, be independent of the starting point (high or low tracer binding). We therefore decided to check that the same binding was achieved after 6 hr of incubation with *d*-tubocurarine and the unlabeled drugs, using membranes that had or had not been preincubated with the tracer before addi-

TABLE 1

"Pseudo-dissociation constants" used to fit the competition curves in the absence or in the presence of *d*-tubocurarine (Figs. 6–10).

Each of the concentrations shown indicates the ligand concentration necessary to occupy 50% of the receptors, as detailed. $K_AK_L/(K_A + K_L)$ measures the ligand concentration necessary to occupy 50% of the receptors at the muscarinic or allosteric site (but not both) (R + L ⇄ RL + LR), α_AK_A measures the ligand concentration necessary to occupy 50% of the [^{3}H]NMS-receptor complex at the accessory site (NR + L ⇄ NRL), $\sqrt{\alpha_{bis}K_AK_L}$ measures the ligand concentration at which the concentration of free receptor is equal to the concentration of receptors occupied at both sites (R + 2L ⇄ LRL), and α_LK_L measures the ligand concentration necessary to occupy 50% of the *d*-tubucurarine-receptor complex muscarinic sites (RD + L ⇄ LRD). All values are given as the best fit value (mean ± standard error; three experiments), except for $\sqrt{\alpha_{bis}K_AK_L}$, where a confidence interval is indicated. α_AK_A and $\sqrt{\alpha_{bis}K_AK_L}$ tend to compensate for each other's effects on the curve fitting; α_AK_A measures the increase of [^{3}H]NMS binding due to occupancy of the accessory site (and induces a shallow competition curve) and $\alpha_{bis}K_AK_L$ measures the decrease of [^{3}H]NMS binding due to occupancy of both binding sites (and induces steep competition curves). To estimate the confidence interval of $\sqrt{\alpha_{bis}K_AK_L}$, we searched for the minimum value that allowed curve fitting of at least one of the competition curves, using the "smallest" (average − 3 SE) α_AK_A value, and the maximum value that allowed curve fitting of at least one of the competition curves, using the "largest" (average + 3 SE) α_AK_A value.

	$K_AK_L/(K_A + K_L)$	α_AK_A	$\sqrt{\alpha_{bis}K_AK_L}$	α_LK_L
d-Tubocurarine	0.72 ± 0.13 μM[a]	2.5 ± 0.22 μM[a]	Large	Large
Gallamine	5.4 ± 0.9 nM	330 ± 91 nM	Large	Large
Methoctramine	3.3 ± 0.5 nM	550 ± 165 nM	40 nM (30–60 nM)	200 ± 75 nM
Bispentamethylene-4-DAMP	32 ± 6 nM	1000 ± 290 nM	300 nM (250–500 nM)	1400 ± 91 nM
Telenzepine	12 ± 2 nM	100 ± 30 μM	Large	60 ± 9 nM
AF-DX 116	90 ± 33 nM	100 ± 33 ±M	Large	640 ± 140 nM
McN-A-343	50%, 0.10 ± 0.03 μM; 50%, 4 ± 1.1 μM	100 ± 35 μM	Large	50%, 1.8 ± 0.7 μM; 50%, 24 ± 8 μM
Dexetimide	0.7 ± 0.2 nM	100 ± 30 μM	Large	6.3 ± 2.5 nM
Levetimide	0.8 ± 0.1 μM	50 ± 15 μM	17 μM (12, large)	4.3 ± 0.18 μM
N-Ethyl-4-DAMP	10 ± 2.4 nM	16 ± 4.5 μM	Large	37 ± 11.2 nM

[a] In the case of *d*-tubocurarine, $K_AK_L/(K_A + K_L)$ is equal to K_D and α_DK_D to α_AK_A.

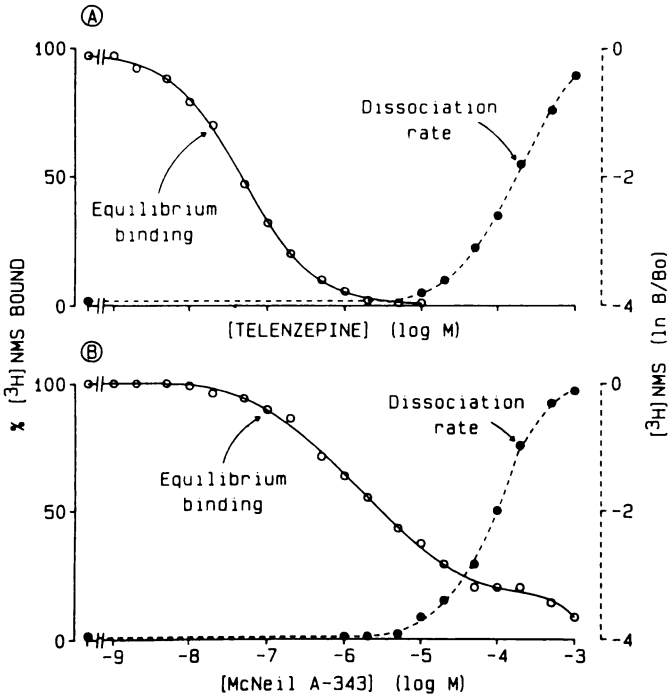

Fig. 2. Dose-effect curves for telenzepine and McN-A-343 effects on [^{3}H] NMS binding (○) and dissociation rate (●). A, Equilibrium binding of 2.0 nM [^{3}H]NMS was measured in the absence or presence of the indicated telenzepine concentrations. The results are compared with the residual [^{3}H]NMS binding, observed 24 min after addition of 1 μM atropine and the indicated telenzepine concentrations. The residual [^{3}H]NMS binding data are plotted on a logarithmic scale, because this is more representative of the dissociation rate constant, k_{off}. The residual tracer binding in the presence of 1 μM atropine alone was 1.8% in this experiment. Data are representative of three experiments. B, As in A, using McNeil-A-343. Data are representative of three experiments.

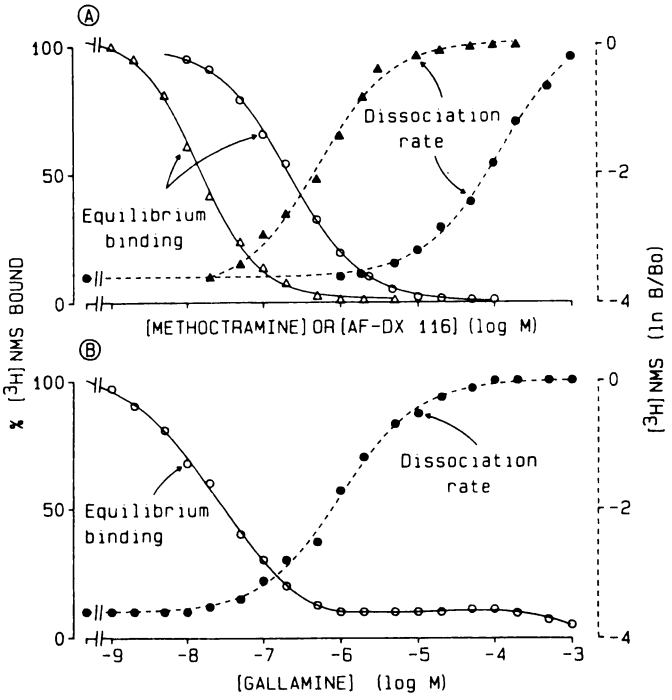

Fig. 3. Dose-effect curves for methoctramine, AF-DX 116, and gallamine effects on [^{3}H]NMS binding (○, △) and dissociation rate (●, ▲). A, As in Fig. 2, measuring equilibrium [^{3}H]NMS binding in the presence of methoctramine (△) or AF-DX 116 (○) and residual [^{3}H]NMS binding 24 min after addition of 1 μM atropine and the indicated methoctramine (▲) or AF-DX 116 (●) concentrations. The residual [^{3}H]NMS binding data are plotted on a logarithmic scale, because this is more representative of the dissociation rate constant, k_{off}. The residual tracer binding in the presence of 1 μM atropine alone was 2% in this experiment. Data are representative of three to five experiments. B, As in Fig. 2, using gallamine. Data are representative of five experiments.

tion of the unlabeled drugs. We preincubated one set of assay tubes with [^{3}H]NMS and the membranes at 25° for 30 min before the addition of 100 μM *d*-tubocurarine and the unlabeled drug. In a second set of assay tubes, we added the tracer, *d*-tubocurarine, and the unlabeled drug simultaneously at the start of the incubation. The level of [^{3}H]NMS binding observed after a second 6-hr incubation was independent of the order of the addition, confirming that equilibrium binding had been achieved (one experiment, without or with four unlabeled drug concentrations, i.e., 1–100 μM gallamine, 0.1–1.0 μM methoctra-

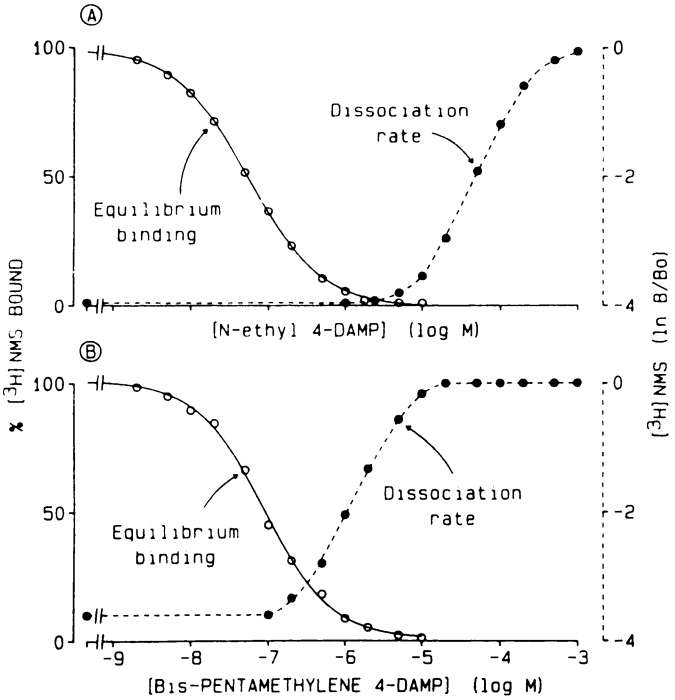

Fig. 4. Dose-effect curves for *N*-ethyl-4-DAMP and bispentamethylene-4-DAMP effects on [^{3}H]NMS binding (○) and dissociation rate (●). The residual [^{3}H]NMS binding data are plotted on a logarithmic scale, because this is more representative of the dissociation rate constant, k_{off}. The residual tracer binding in the presence of 1 μM atropine alone was 1.8% (*N*-ethyl-4-DAMP) (A) or 2% (bispentamethylene-4-DAMP) (B). A, As in Fig. 2, using *N*-ethyl-4-DAMP; B, as in Fig. 2, using bispentamethylene-4-DAMP. Data are representative of five experiments.

mine, 0.5–5.0 μM bispentamethylene-4-DAMP, 5–50 nM telenzepine, 0.5–5.0 μM AF-DX 116, 5–50 μM McNeil-A-343, 2–20 nM dexetimide, 5–50 μM levetimide, or 50–500 nM *N*-ethyl-4-DAMP).

Curve fitting. Our goal was to define, for each compound, the minimum model allowing description of the experimental data. To achieve this goal, we began by determining separately the values of K_N (from the [^{3}H]NMS saturation curve), $\alpha_D K_D$ and $\alpha_A K_A$ (EC_{50} values for the inhibition of tracer dissociation by *d*-tubocurarine and by the compound, respectively), and α_D and K_D (from the [^{3}H]NMS/*d*-tubocurarine competition curve).

The simplest model assumes that *d*-tubocurarine and the competitor compete for the same accessory site on the receptor. Equation 3 then simplifies to

$$K'_N = K_N \left\{ \frac{1 + L/K_A + D/K_D}{1 + \frac{L}{\alpha_A K_A} + \frac{D}{\alpha_D K_D}} \right\} \quad (5)$$

This model allowed us to easily fit the gallamine competition curves obtained at different *d*-tubocurarine concentrations (Fig. 6 and results not shown). The values of K_A and $\alpha_A K_A$ are summarized in Table 1. The gallamine IC_{35} increased linearly with increasing *d*-tubocurarine concentrations, as expected if both compounds compete for the same (accessory) site on muscarinic receptors.

We attempted to use the same equation to describe the bispentamethylene-4-DAMP and methoctramine competition curves in the absence and presence of *d*-tubocurarine. This model was, however, unsatisfactory, because we had to use K_D and $\alpha_D K_D$ values of 5 and 20 μM, respectively (as opposed to the experimentally determined values of 0.7 and 2.5 μM), to describe the effect of 100 μM *d*-tubocurarine on binding. Furthermore, the "best-fit" K_D and $\alpha_D K_D$ values corresponding to each competition curve increased with increasing *d*-tubocurarine concentrations. We therefore rejected this model.

As shown in Figs. 7 and 8, the IC_{35} of bispentamethylene-4-DAMP and methoctramine increased nonlinearly with increasing *d*-tubocurarine concentrations. At concentrations above 30 μM, when *d*-tubocurarine is expected to saturate the accessory site, the IC_{35} values of the two drugs reached maximum values of about 10 times the control values. We therefore assumed that *d*-tubocurarine, when binding to the accessory site, inhibited but did not prevent binding of bispentamethylene-4-DAMP or methoctramine to the muscarinic receptor. This is described by eq. 6.

$$K'_N = K_N \frac{1 + \frac{L}{K_L} + \frac{L}{K_A} + \frac{D}{K_D} + \frac{L \cdot D}{\alpha_L K_L K_D}}{1 + \frac{D}{\alpha_D K_D} + \frac{L}{\alpha_A K_A}} \quad (6)$$

The fit obtained with this equation was much more satisfactory, compared with eq. 5. Nevertheless, in both cases the experimental competition curves were steeper than curves expected from eq. 6. The curve fitting was improved by allowing "double occupancy" (simultaneous binding to the accessory and muscarinic sites) by the drug, as described by the complete eq. 3 (see Experimental Procedures). The parameters used for curve-fitting are summarized in Table 1.

The competition curves obtained with telenzepine, McNeil-A-343, AF-DX 116, *N*-ethyl-4-DAMP, dexetimide, and levetimide were barely shifted, if at all, in the presence of *d*-tubocurarine (Figs. 9 and 10). This result suggested that all of these compounds recognize the muscarinic site and have similar affinities for the free receptor (K_L) and for the *d*-tubocurarine-occupied receptor ($\alpha_L K_L$). Just as for methoctramine and bis-

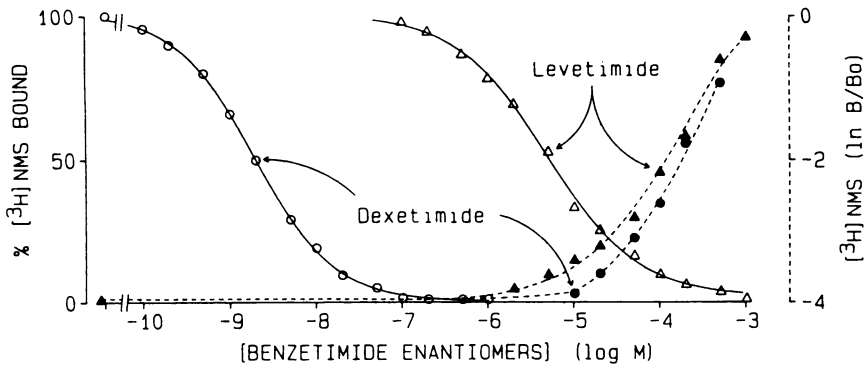

Fig. 5. Dose-effect curves for the effects of the benzetimide enantiomers dexetimide (○, ●) and levetimide (△, ▲) on [^{3}H]NMS binding (○, △) and dissociation rate (●, ▲). The residual [^{3}H]NMS binding data are plotted on a logarithmic scale, because this is more representative of the dissociation rate constant, k_{off}. The residual tracer binding in the presence of 1 μM atropine alone was 1.8% in this experiment. The experiments were as in Fig. 2, using either dexetimide or levetimide. Data are representative of three experiments.

TABLE 2

Description of the competition and dose-effect curves

This table summarizes the values of the drug concentration inhibiting [^{3}H]NMS binding by 50% (IC_{50}) and the Hill coefficient of the competition curves shown in Figs. 1–5, as well as the values of the drug concentration decreasing the [^{3}H]NMS dissociation rate by a factor 2 (EC_{50}) and the Hill coefficient of the dose-effect curves shown in Figs. 1–5.

	IC_{50} (n_H)[a]	EC_{50} (n_H)[b]
d-Tubocurarine	>500 μM (0.5)	3.0 μM (1.0)
Telenzepine	50 nM (0.93)	160 μM (1.1)
McN-A-343	3.0 μM (0.5)	100 μM (1.2)
Methoctramine	16 nM (1.2)	0.5 μM (1.1)
AF-DX 116	210 nM (0.9)	100 μM (0.9)
Gallamine	33 nM (0.7)	0.9 μM (0.9)
N-Ethyl-4-DAMP	40 nM (1.0)	16 μM (1.2)
Bispentamethylene-4-DAMP	100 nM (1.0)	1.3 μM (1.3)
Dexetimide	2.1 nM (1.0)	100 μM (1.2)
Levetimide	6.0 μM (0.8)	50 μM (1.2)

[a] The standard deviation of the log (IC_{50}) was always less than ±0.1 log unit (i.e., 79–126% of the average value). The standard deviation of the Hill coefficient of the competition curve was below ±0.1.

[b] The standard deviation of the log (IC_{50}) was always less than ±0.2 log unit (63–158% of the average value). The standard deviation of the Hill coefficient of the dose-effect curve for slowing the [^{3}H]NMS dissociation was always lower than ±0.2.

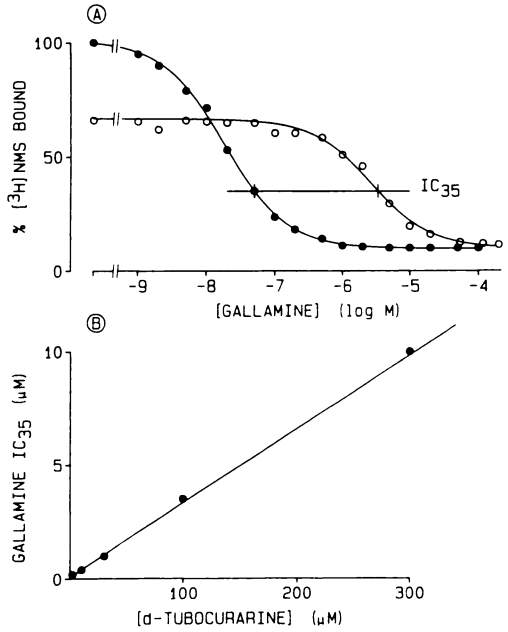

Fig. 6. Effect of *d*-tubocurarine on gallamine competition curves. A, [^{3}H] NMS (2.0 nM) binding was measured in the absence or presence of the indicated *d*-tubocurarine concentrations and in the absence (●) or presence (○) of 100 μM *d*-tubocurarine. Data are the average of five experiments. B, The concentration of gallamine necessary to reduce [^{3}H]NMS binding to 35% of control (in the absence of unlabeled drug) was measured at different *d*-tubocurarine concentrations (shown in A at 0 and 100 μM). Data are representative of three experiments.

pentamethylene-4-DAMP, the calculated levetimide competition curve was too shallow unless we allowed simultaneous binding to the muscarinic and accessory sites. A good fit to the experimental curve could, however, be achieved by using the upper limit of the $\alpha_A K_A$ value rather than the experimental average $\alpha_A K_A$ value. The parameters used for curve fitting are summarized in Table 1.

Inhibition of [^{3}H]NMS binding by McNeil-A-343 was fully detectable in the presence of *d*-tubocurarine (Fig. 9). This result suggested that McNeil-A-343 preferentially recognizes the muscarinic site. It was completely possible to fit the McNeil-A-343 competition curves in the absence and in the presence of *d*-tubocurarine. The number of parameters necessary for curve fitting was, however, very large, because (like other muscarinic agonists) McNeil-A-343 discriminated two receptor states (with high and low affinity). If we assumed that the proportion of high/low affinity states (50%) was unchanged in the presence of *d*-tubocurarine, then the McNeil-A-343 competition curves could be fitted with K_L values of 0.1 and 4.0 μM in the absence of *d*-tubocurarine and $\alpha_L K_L$ values of 1.8 and 24 μM, respectively, for the *d*-tubocurarine-occupied receptors (Table 1).

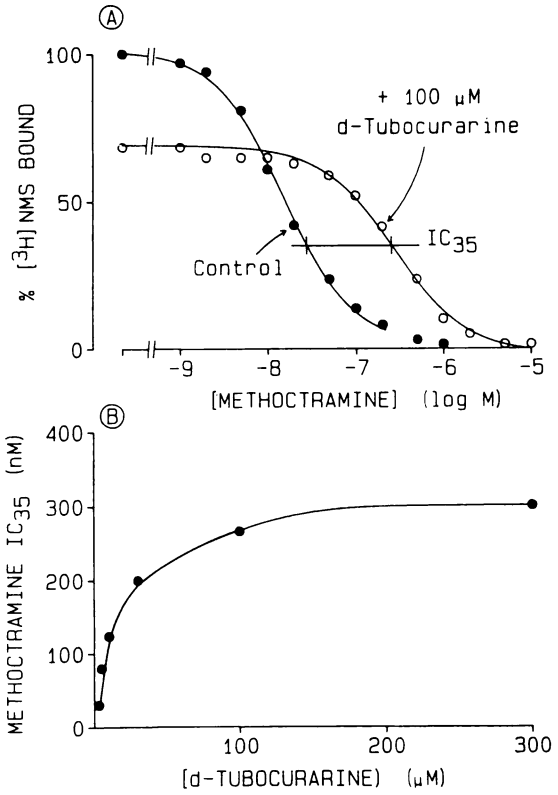

Fig. 7. Effect of *d*-tubocurarine on methoctramine competition curves. Experiments were as in Fig. 6, using methoctramine instead of gallamine. A, Average of four experiments; B, average of two experiments.

Discussion

Ellis and Seidenberg investigated the effect of several compounds on the [^{3}H]NMS dissociation rate. They demonstrated that "any two allosteric modulators interact at a common site on the muscarinic receptor" (15, p. 639), and they identified the region of the receptor that is responsible for the subtype selectivity of gallamine binding (21). Unfortunately, their experimental design did not allow estimation of the affinities of the compounds for the free receptor or identification of the binding site (muscarinic or accessory site) that is recognized preferentially by these compounds.

We previously demonstrated that *d*-tubocurarine is a pure allosteric antagonist at cardiac M_2 receptors; it markedly slowed, but did not prevent, [^{3}H]NMS association with and dissociation from the receptor (11). We therefore decided to use this compound as a probe to identify other compounds that preferentially recognize the allosteric site. We assumed that *d*-tubocurarine occupation of the accessory site would prevent

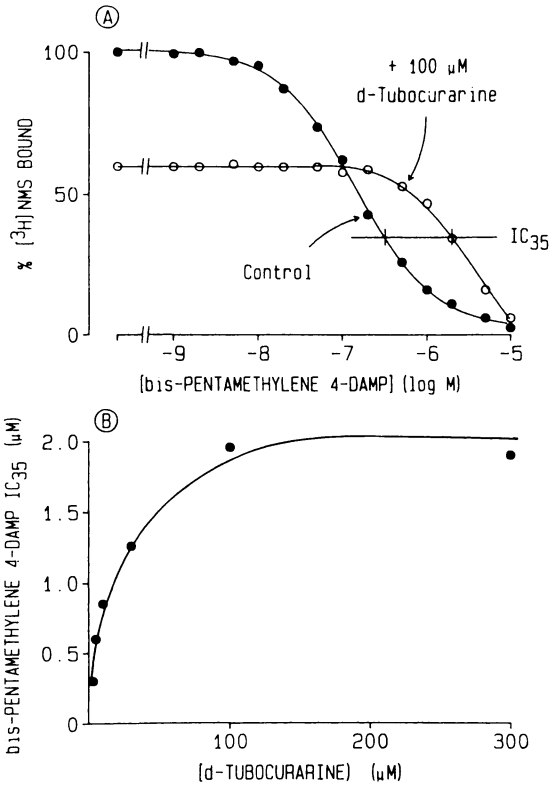

Fig. 8. Effect of *d*-tubocurarine on bispentamethylene-4-DAMP competition curves. Experiments were as in Fig. 6, using bispentamethylene-4-DAMP instead of gallamine. A, Average of four experiments; B, average of two experiments.

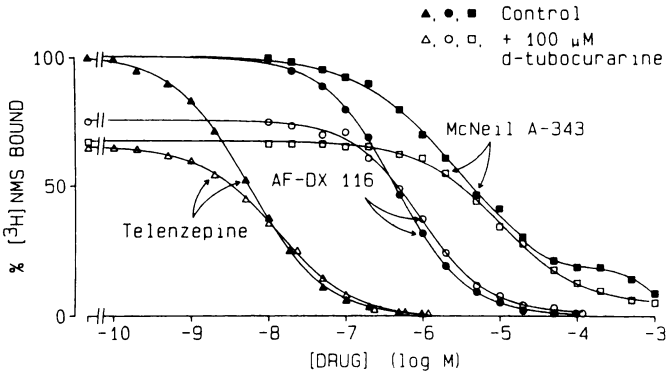

Fig. 9. Effect of *d*-tubocurarine on telenzepine, AF-DX 116, and McN-A-343 competition curves. [^{3}H]NMS (2.0 nM) binding was measured in the absence (▲, ●, ■) or presence (△, ○, □) of 100 μM *d*-tubocurarine and in the absence or presence of the indicated concentrations of telenzepine (△, ▲), AF-DX 116 (○, ●), or McNeil-A-343 (■, □). Data are averages of three experiments.

receptor recognition by allosteric compounds but would very minimally alter drug binding to the muscarinic site itself. As a result, [^{3}H]NMS binding inhibition by allosteric drugs should be relieved by *d*-tubocurarine, whereas [^{3}H]NMS binding inhibition by muscarinic ligands should be little affected.

This concept is illustrated in Figs. 6 and 9. Gallamine binding to the accessory site was competitively inhibited by *d*-tubocurarine, and the IC_{35} increased linearly with increasing *d*-tubocurarine concentrations (Fig. 6). In contrast, telenzepine recognized the empty and *d*-tubocurarine-occupied receptors with very similar affinities, and inhibition of [^{3}H]NMS binding by

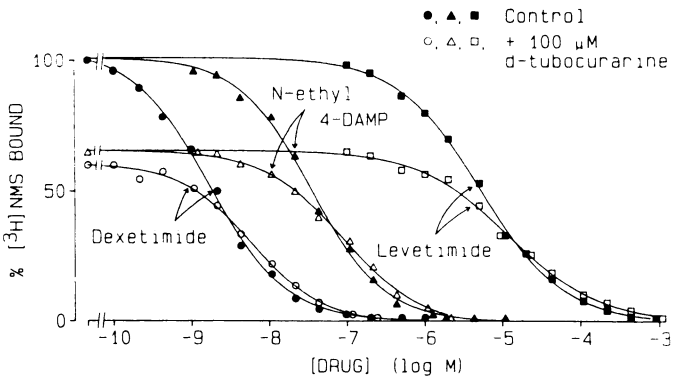

Fig. 10. Effect of *d*-tubocurarine on the dexetimide, levetimide, and *N*-ethyl-4-DAMP competition curves. [^{3}H]NMS (2.0 nM) binding was measured in the absence (●, ▲, ■) or presence (○, △, □) of 100 μM *d*-tubocurarine and in the absence or presence of the indicated concentrations of dexetimide (○, ●), levetimide (■, □), or *N*-ethyl-4-DAMP (△, ▲). Data are the average of three experiments.

telenzepine was not affected by the presence of *d*-tubocurarine (Fig. 9).

The competitors studied here were chosen as follows. 1) We wanted to include compounds that probably prefer the muscarinic site, as well as allosteric compounds, to ensure that our method is discriminant. Gallamine and McN-A-343, like *d*-tubocurarine, do not completely inhibit [^{3}H]NMS binding at equilibrium. We therefore considered these compounds as likely allosteric drugs. We also included methoctramine and bispentamethylene-4-DAMP, because at relatively low concentrations they inhibit [^{3}H]NMS dissociation. In contrast, the two benzetemide enantiomers (dexetimide and levetimide) are strongly discriminated by the muscarinic receptors but decrease [^{3}H]NMS dissociation at similar (millimolar) concentrations. We therefore thought that they are both competitive antagonists, with at most a weak affinity for the accessory site. 2) Because many putative allosteric drugs are subtype selective, we also included the selective compounds telenzepine, AF-DX 116, and *N*-ethyl-4-DAMP. For technical reasons we chose to induce the tracer dissociation by addition of an unlabeled drug rather than by chemical dilution. At 1 μM, atropine completely inhibited [^{3}H]NMS binding, but at least 10-fold higher concentrations were necessary to slow [^{3}H]NMS dissociation (the atropine EC_{50} value was >100 μM). This suggested that the accessory site is not recognized by 1 μM atropine. We therefore systematically included 1 μM atropine when investigating the effects of other unlabeled drugs on the [^{3}H]NMS dissociation rate.

Effect of the drugs on [^{3}H]NMS binding and [^{3}H]NMS dissociation. As shown in Figs. 1–5, there was no correlation between the drug potencies for [^{3}H]NMS binding inhibition and for [^{3}H]NMS dissociation inhibition. All of the compounds with a single positive charge decreased the [^{3}H]NMS dissociation rate at very high concentrations (EC_{50} in the 100 μM range). The compounds with two or more positive charges were up to 400-fold more potent (EC_{50} in the micromolar range).

Decreasing the tracer dissociation rate promotes tracer binding. The shallow competition curves obtained with McN-A-343, gallamine, levetimide, and *d*-tubocurarine result at least in part from the combination of inhibitory and facilitating effects of the drugs on [^{3}H]NMS binding. In contrast, telenzepine, AF-DX 116, *N*-ethyl-4-DAMP, and dexetimide completely inhibited tracer binding at concentrations that did not

affect the tracer dissociation rate, and the competition curves were therefore normal. We expected (but did not observe) shallow competition curves for bispentamethylene-4-DAMP and methoctramine.

d-Tubocurarine did not prevent tracer binding inhibition by any of the single-charge compounds (including McN-A-343 and levetimide). In contrast, the methoctramine, gallamine, and bispentamethylene-4-DAMP competition curves were markedly shifted in the presence of *d*-tubocurarine.

The gallamine competition curves, in the absence and presence of *d*-tubocurarine, were easily fitted by assuming that both compounds compete for the same accessory site and modify but do not prevent [^{3}H]NMS binding to the muscarinic site. We found no evidence that gallamine recognizes the muscarinic site ($\alpha_L K_L$ and $\alpha_{bis} K_A K_L$ were large).

Binding of telenzepine, AF-DX 116, dexetimide, levetimide, *N*-ethyl-4-DAMP, and (probably) McN-A-343 to the *d*-tubocurarine-receptor complex ($\alpha_L K_L$) was quite good, compared with binding to the empty receptor [$K_A K_L/(K_A + K_L)$]. On the other hand, all of these compounds had a much weaker affinity for the NMS*-receptor complex ($\alpha_A K_A \gg \alpha_L K_L$). We therefore believe that they all competitively recognize the muscarinic binding site and have a very weak affinity for the accessory site ($K_L \ll K_A$). If this is correct, then the ratio $K_A K_L/(K_A + K_L)$ is equal to K_L, and the value of α_L can be obtained from Table 1. Using these assumptions, we obtained α_L values ranging between 3.7 (*N*-ethyl-4-DAMP) and 9 (dexetimide) for several muscarinic antagonists. This suggests that all of the antagonists decrease to the same extent the affinity of *d*-tubocurarine for the accessory site.

Binding of methoctramine and bispentamethylene-4-DAMP to the *d*-tubocurarine-receptor complex was weak, compared with binding to the empty receptor ($\alpha_L K_L > K_A$ or K_L), but was comparable to binding to the NMS-receptor complex ($\alpha_L K_L \approx \alpha_A K_A$). Furthermore, the curve fitting was significantly better if we included a finite value for $\alpha_{bis} K_A K_L$, i.e., allowed for receptor recognition by two ligands, one at the muscarinic site and one at the accessory site. We would therefore like to suggest that methoctramine and bispentamethylene-4-DAMP had, in this incubation buffer, rather comparable affinities for the accessory site and for the muscarinic site ($K_A \approx K_L$). This does not necessarily mean that both compounds significantly recognize the accessory site in a "physiological buffer"; indeed, for this study we chose a low ionic strength buffer (devoid of bivalent ions) to facilitate the recognition of the allosteric site.

In conclusion, comparison of [^{3}H]NMS binding inhibition in the absence and presence of *d*-tubocurarine allowed us to distinguish one compound (gallamine) that preferentially recognized the accessory site, six compounds that probably preferred the muscarinic site, and two compounds that were apparently able to recognize both binding sites. The presence of several positive charges on the compounds facilitated recognition of the accessory site but did not prevent recognition of the muscarinic site.

References

1. Bonner, T. I. The molecular basis of muscarinic receptor diversity. *Trends Neurosci.* **12**:148–151 (1989).
2. Stockton, J. M., N. J. M. Birdsall, A. S. V. Burgen, and E. C. Hulme. Modification of the binding properties of muscarinic receptors by gallamine. *Mol. Pharmacol.* **23**:551–557 (1983).
3. Birdsall, N. J. M., E. C. Hulme, W. Kromer, and J. M. Stockton. A second drug-binding site on muscarinic receptors. *Fed. Proc.* **48**:2525–2527 (1987).
4. Flynn, D. D., A. A. Vaishnav, and D. C. Mash. Interactions of cocaine with primary and secondary recognition sites on muscarinic receptors. *Mol. Pharmacol.* **41**:736–742 (1992).
5. Giraldo, E., R. Micheletti, E. Montagna, A. Giachetti, M. A. Vigano, H. Ladinsky, and C. Melchiorre. Binding and functional characterization of the cardioselective muscarinic antagonist methoctramine. *J. Pharmacol. Exp. Ther.* **244**:1016–1020 (1988).
6. Roffel, A. F., C. R. S. Elzinga, H. Meurs, and J. Zaagsma. Allosteric interactions of three muscarinic antagonists at bovine tracheal smooth muscle and cardiac M_2 receptors. *Eur. J. Pharmacol.* **172**:61–70 (1989).
7. Cohen-Armon, M., Y. I. Henis, Y. Kloog, and M. Sokolovsky. Interactions of quinidine and lidocaine with rat brain and heart muscarinic receptors. *Biochem. Biophys. Res. Commun.* **127**:326–332 (1985).
8. Waelbroeck, M., P. De Neef, P. Robberecht, and J. Christophe. Inhibitory effects of quinidine on rat heart muscarinic receptors. *Life Sci.* **35**:1069–1076 (1984).
9. Gillard, M., F. Brunner, M. Waelbroeck, M. Svoboda, and J. Christophe. Bretylium tosylate binds preferentially to muscarinic receptors labelled with [^{3}H]oxotremorine M (SH or 'high affinity' receptors) in rat heart and brain cortex. *Eur. J. Pharmacol.* **160**:117–124 (1989).
10. Eglen, R. M., A. D. Michel, C. M. Cornett, E. A. Kunysz, and R. L. Whiting. The interaction of hexamethonium with muscarinic receptor subtypes *in vitro*. *Br. J. Pharmacol.* **98**:499–506 (1989).
11. Waelbroeck, M., P. Robberecht, P. De Neef, and J. Christophe. Effects of *d*-tubocurarine on rat cardiac muscarinic receptors: a comparison with gallamine. *J. Recept. Res.* **8**:787–808 (1988).
12. Nedoma, J., S. Tucek, A. F. Danilov, and S. A. Shelkovnikov. Stabilization of antagonist binding to cardiac muscarinic acetylcholine receptors by gallamine and other neuromuscular blocking drugs. *J. Pharmacol. Exp. Ther.* **236**:219–223 (1985).
13. Kloog, Y., and M. Sokolovsky. Bisquaternary pyridinium oximes as allosteric inhibitors of rat brain muscarinic receptors. *Mol. Pharmacol.* **27**:418–428 (1985).
14. Flynn, D. D., and D. C. Mash. Multiple *in vitro* interactions with and differential *in vivo* regulation of muscarinic receptor subtypes by tetrahydroaminoacridine. *J. Pharmacol. Exp. Ther.* **250**:573–581 (1989).
15. Ellis, J., and M. Seidenberg. Two allosteric modulators interact at a common site on cardiac muscarinic receptors. *Mol. Pharmacol.* **42**:638–641 (1992).
16. Waelbroeck, M., P. Robberecht, P. De Neef, and J. Christophe. Effects of verapamil on the binding properties of rat heart muscarinic receptors: evidence for an allosteric site. *Biochem. Biophys. Res. Commun.* **121**:340–345 (1984).
17. Lai, W. S., V. Ramkumar, and E. E. El-Fakahany. Possible allosteric interaction of 4-aminopyridine with rat brain muscarinic acetylcholine receptors. *J. Neurochem.* **44**:1936–1942 (1985).
18. Hu, J., S.-Z. Wang, C. Forray, and E. E. El-Fakahany. Complex allosteric modulation of cardiac muscarinic receptors by protamine: potential model for putative endogenous ligands. *Mol. Pharmacol.* **42**:311–324 (1992).
19. Max, S. I., J.-S. Liang, and L. T. Potter. Purification and properties of m1-toxin, a specific antagonist of m1 muscarinic receptors. *J. Neurosci.* **13**:4293–4300 (1993).
20. Birdsall, N. J. M., A. S. V. Burgen, E. C. Hulme, J. M. Stockton, and M. J. Zigmond. The effect of McN-A-343 on muscarinic receptors in the cerebral cortex and heart. *Br. J. Pharmacol.* **78**:257–259 (1983).
21. Ellis, J., M. Seidenberg, and M. R. Brann. Use of chimeric muscarinic receptors to investigate epitopes involved in allosteric interactions. *Mol. Pharmacol.* **44**:583–588 (1993).

Send reprint requests to: M. Waelbroeck, Department of Biochemistry and Nutrition, Medical School, Université Libre de Bruxelles, Building G/E, CP 611, 808 Route de Lennik, B-1070 Brussels, Belgium.